Mo, W, and Fe EXAFS of the $[Cl_2FeS_2MS_2FeCl_2]^{2-}$ (M = Mo, W) Dianions. A Comparison with the Mo EXAFS of Nitrogenase

Boon K. Teo,*§ Mark R. Antonio,† D. Coucouvanis,*‡ E. D. Simhon,‡ and P. P. Stremple‡

Contribution from Bell Laboratories, Murray Hill, New Jersey 07974, Department of Chemistry, Michigan State University, East Lansing, Michigan 48824, Sohio, Cleveland, Ohio 44128, and Department of Chemistry, University of Iowa, Iowa City, Iowa 52242.
Received January 19, 1982

Abstract: The Mo, W, and Fe EXAFS of $(Ph_4P)_2[Cl_2FeS_2MS_2FeCl_2]$ (M = Mo or W) are reported. The M-S, M-Fe, and Fe-S(Cl) distances as determined by M (M = Mo, W) and Fe EXAFS agree with the crystallographic values to better than 0.5%. The numbers of neighboring atoms (around the Mo, W, and Fe) also agree with the crystallographic values to better than 9% (with one exception). A comparison of the Fourier transforms of the Mo EXAFS of $[S_2MoS_2Fe(SPh)_2]^{2-}$, $[Cl_2FeS_2MoS_2FeCl_2]^{2-}$ (this work), and $[Mo_2Fe_6S_9(SEt)_8]^{3-}$ with that of the MoFe protein of nitrogenase is made. The former three-model complexes contain one, two, and three iron atoms in the second coordination sphere around the Mo atom(s). The Fourier transform of the Mo EXAFS of the MoFe protein of nitrogenase is quite different than the corresponding transforms from the model complexes, at least as far as peak intensities are concerned. Qualitatively Mo-S and Mo-Fe peaks in the Fourier transform of the MoFe protein data resemble the corresponding peaks in the transforms of the EXAFS data for the double-cubane clusters and the title compound (M = Mo), respectively. The Mo-Fe distance in the title compound (2.76 Å) is similar to that found in the MoFe protein of nitrogenase (2.71 Å). By contrast, the Mo-S bond length in the title compound is significantly shorter than the Mo-S values reported for the MoFe protein (2.35 Å) and the $[Mo_2Fe_6S_9(SEt)_8]^{3-}$ "double cubane" (2.340 Å). The latter contains a six-coordinate molybdenum in a +3.5 formal oxidation state.

Molybdenum K-edge extended X-ray absorption fine structure (EXAFS) analyses have been reported for the MoFe protein components of *Clostridium pasteurianum*[1] and *Azotobacter vinelandii*[2] (Av) nitrogenases and for the Fe-Mo cofactor[2] (FeMo-co) from Av.[3] These studies suggest that the Mo site in the MoFe protein of nitrogenase has three or four sulfur atoms at ca. 2.36 ± 0.02 Å, one or two sulfur atoms at 2.49 ± 0.03 Å, and two or three iron atoms at 2.71 ± 0.03 Å as nearest neighbors.[1,4,5] EXAFS studies have been performed on two types of synthetic model compounds: the double cubanes $[Mo_2Fe_6S_9(SEt)_8]^{3-}$,[5-7] $[Mo_2Fe_6S_8(SEt)_9]^{3-}$,[5b,7] $[Mo_2Fe_6S_8(SEt)_3(OPh)_6]^{3-}$,[7] and the single cubane $[MoFe_4S_4(SEt)_3(C_6H_4O_2)_3]^{3-}$,[8] and the Mo-Fe-S clusters that contain MoS_4^{2-} as a chelating ligand,[6,8,9] $[(PhS)_2FeS_2MoS_2]^{2-}$[9,10] and $[S_2MoS_2FeS_2MoS_2]^{3-}$.[9,11] In the former type of complexes each molybdenum has three iron atoms as nearest neighbors, whereas in the latter type there is only one iron atom near the Mo atom. Herein we report on the Mo and Fe K-edge and on the W L_3-edge EXAFS of the Ph_4P^+ salts of the $[Cl_2FeS_2MS_2FeCl_2]^{2-}$ dianions (M = Mo, **1**; M = W, **2**). The dianions **1** and **2** represent the only examples among the Mo-Fe-S complexes that contain two Fe atoms around the Mo (or W) and have been characterized structurally by X-ray diffraction methods.[12,13]

Data Collection

Compounds **1** and **2** were prepared according to literature methods.[12,13]

The X-ray absorption measurements were performed at the Cornell High Energy Synchrotron Source (CHESS) with use of the C2 (EXAFS) beam line.[14] The synchrotron radiation from the Cornell Electron Storage Ring (CESR) at the Wilson Laboratory of Cornell University, after passing through a first set of slits, was monochromated by a channel-cut silicon ⟨220⟩ crystal. A second set of slits which resides in the experimental station was used to shape the X-ray beam size to 1 × 12 mm. The X-ray beam intensity (I_0) was reduced by 50% (by slightly detuning the monochromator) before each run which corresponds to a 98% rejection of harmonics ($\lambda/2$) at a photon energy of 20 keV (Mo K-edge).[15] CESR was operating at 5.18 GeV with approximately 4-12 mA of stored beam current.

The experiments were done in transmission mode on boron nitride pellets prepared under nitrogen. The monochromated X-ray beam passes through a first ionization chamber (8 cm), which measures the incident beam intensity I_0, then through the sample, and finally through another ionization chamber (30 cm), which measures the transmitted intensity I. Argon was the detecting gas used in both ionization chambers (flow-type) for the Mo K-edge, while nitrogen and argon were used in the I_0 and I ionization chambers, respectively, for both W L_3-edge and Fe K-edge. The EXAFS spectra were recorded with an integration time of 1-2 s/point (constant I_0 accumulation) with 150, 200, and 215 steps covering about 900 eV above the edge for Mo (19 900-20 900 eV), W (10 100-11 000 eV), and Fe (7010-7910 eV), respectively. The raw data, as a function of photon energy, E, were taken in constant k steps which amounted to 3, 2, and 2 eV/point at the beginning and 10, 6, and 6 eV/point at the end of the scan for Mo, W, and Fe, respectively. The ordinates of the spectra were computed by taking $\mu x = \ln(I_0/I)$ where μ is the total absorption and x is the sample thickness.

§ Bell Laboratories.
† Michigan State University and Sohio.
‡ University of Iowa. Present address: University of Michigan.

(1) Cramer, S. P.; Hodgson, K. O.; Gillum, W. O.; Mortenson, L. E. *J. Am. Chem. Soc.* **1978**, *100*, 3398.
(2) Cramer, S. P.; Gillum, W. O.; Hodgson, K. O.; Mortenson, L. E.; Stiefel, E. I.; Chisnell, J. R.; Brill, W. J.; Shah, V. K. *J. Am. Chem. Soc.* **1978**, *100*, 3814.
(3) Shah, V. K.; Brill, W. J. *Proc. Natl. Acad. Sci. U.S.A.* **1977**, *74*, 3249.
(4) Teo, B. K.; Averill, B. A. *Biochem. Biophys. Res. Commun.* **1979**, *88*, 1454.
(5) (a) Wolff, T. E.; Berg, J. M.; Warrick, C.; Hodgson, K. O.; Holm, R. H.; Frankel, R. B. *J. Am. Chem. Soc.* **1978**, *100*, 4630. (b) Wolff, T. E.; Berg, J. M.; Hodgson, K. O.; Frankel, R. B.; Holm, R. H. *Ibid.* **1979**, *101*, 4140.
(6) Newton, W. E.; McDonald, J. W.; Friesen, G. D.; Burgess, B. K.; Conradson, S. D.; Hodgson, K. O. In "Current Perspectives in Nitrogen Fixation"; Gibson, A. H. Newton, W. E., Eds.; Australian Academy of Science: Canberra, 1981; pp 30-39.
(7) Antonio, M. R.; Teo, B. K.; Cleland, W. E.; Averill, B. A. *J. Am. Chem. Soc.* **1983**, *105*, 3477.
(8) Burgess, B. K.; Yang, S. S.; You, C. B.; Li, J. G.; Friesen, G. D.; Pan, W. H.; Stiefel, E. I.; Newton, W. E.; Conradson, S. R.; Hodgson, K. O. In "Current Perspectives in Nitrogen Fixation"; Gibson, A. H., Newton, W. E., Eds.; Australian Academy of Science: Canberra, 1981; pp 71-74.
(9) Teo, B. K.; Antonio, M. R.; Averill, B. A. *J. Am. Chem. Soc.* **1983**, *105*, 3751.
(10) (a) Tieckelmann, R. H.; Silvis, H. C.; Kent, T. A.; Huynh, B. H.; Waszczak, J. V.; Teo, B. K.; Averill, B. A. *J. Am. Chem. Soc.* **1980**, *102*, 5550. (b) Coucouvanis, D.; Simhon, E. D.; Swenson, D.; Baenziger, N. C. *J. Chem. Soc., Chem. Commun.* **1979**, 361.
(11) Coucouvanis, D.; Simhon, E. D.; Baenziger, N. C. *J. Am. Chem. Soc.* **1980**, *102*, 6644.
(12) Coucouvanis, D.; Baenziger, N. C.; Simhon, E. D.; Stremple, P.; Swenson, D.; Simopoulos, A.; Kostikas, A.; Petrouleas, V.; Papaefthymiou, V. *J. Am. Chem. Soc.* **1980**, *102*, 1732.
(13) Coucouvanis, D., et al. *J. Am. Chem. Soc.*, submitted.
(14) Batterman, B. W.; Ashcroft, N. W. *Science* **1979**, *206*, 157.
(15) Mills, D.; Pollock, V. *Rev. Sci. Instrum.* **1980**, *51*, 1664.

0002-7863/83/1505-5767$01.50/0

Table I. The BFBT Least-Squares Refined Interatomic Distances (r, Å), Debye-Waller Factors (σ, Å), and Coordination Numbers (N) with Fitting Errors (in Parentheses; Excluding Systematic Errors Such as Background Removal, Fourier Filtering, Truncation, etc.), Energy Threshold Differences ($\Delta E_0{}^p$, eV), and Scale Factors (B) for $[Cl_2FeS_2MS_2FeCl_2]^{2-}$ where M = Mo (1) or W (2), Along with Available Single-Crystal X-ray Diffraction Results

		distance				coordination number			
		EXAFS		diffraction[b]		EXAFS			
compd no.	A-B[a]	$\Delta E_0{}^p$	r	r	% error	σ	B	N	% error
1[c]	Mo-S	7.20	2.237 (9)	2.204 (5)	1.5	0.043 (10)	2.313	3.8 (5)	−5.8
		7.16	2.237			0.043	2.292	3.7	−6.7
	Mo-Fe	−4.00	2.769 (35)	2.775 (6)	−0.2	0.065 (23)	0.810	1.5 (7)	−23.3
		−3.84	2.770			0.078	1.146	2.4	20.1
1[d]	Fe-S/Cl	8.16	2.271 (17)	2.260 (4)	0.5	0.050 (16)	1.891	3.7 (8)	−8.7
		8.04	2.271			0.051	1.902	3.7	−7.5
	Fe-Mo	−7.26	2.768 (41)	2.775 (6)	−0.3	0.075 (30)	0.622	1.4 (11)	44.2
		−6.73	2.771			0.067	0.475	1.0	3.6
2[e]	W-S	14.62	2.222 (8)	2.209 (5)	0.6	0.028 (20)	1.836	2.9 (4)	−28.6
		14.48	2.222			0.028	1.823	2.8	−30.1
	W-Fe	−1.53	2.760 (33)	2.801 (9)	−0.2	0.063 (24)	0.700	1.8 (8)	−7.6
		−1.57	2.760			0.073	0.911	2.7	35.4
2[d,f]	Fe-S/Cl	4.05	2.266 (25)	2.280 (5)	−0.6	0.063 (20)	1.946	4.1 (12)	2.9
	Fe-W	7.54	2.821 (65)	2.801 (9)	0.7	0.074 (15)	0.487	1.1 (2)	11.9

[a] Each backscattering term is represented by A-B where A is the absorber and B the backscatterer. The parameters in the second row of each term (except 2, see footnote *f*) were obtained from a restricted fit with the ratio of the scale factors for the two backscattering terms fixed at the known value. [b] References 12 and 13. Where applicable the esd's were computed as follows: $s = \sigma = [\Sigma^N_{i=1}(x - \bar{x})^2/(N-1)]^{1/2}$, where $\bar{x}_i$ is the length of the bond and $\bar{x}$ is the mean value for the N equivalent bond lengths. [c] Mo K-edge. [d] Fe K-edge. [e] W L_3-edge. [f] The ratio of the scale factors is restricted to the known value of Fe-S/Cl:Fe-W = 4:1 to alleviate fitting problems due to the small contribution of the Fe-W backscattering to the total EXAFS.

Data Analysis

For EXAFS analysis, it is necessary to convert the photon energy E into photoelectron wave vector $k = [(2m/\hbar^2)(E - E_0)]^{1/2}$ where E_0 is the energy threshold and m is the mass of an electron. The energy threshold, E_0, was chosen at 19980, 10210, and 7130 eV for Mo, W, and Fe, respectively. The edge positions, $E_0{}^p$, are 19984 and 7117 eV for the Mo and Fe edges of **1** and 10198 and 7115 eV for the W and Fe edges of **2**. After conversion of E into photoelectron wave vector k, the data were multiplied by k^3 and the modulation of the absorption coefficient, the EXAFS $\chi(k) = (\mu - \mu_0)/\mu_0$, was obtained by removing a cubic spline background fit to the data with four sections each of Δk = 3.5 Å^{-1} and normalized with the edge jump and corrected for the μ_0 dropoff via Victoreen's true absorption. Fourier transforms of the $k^3\chi(k)$ vs. k EXAFS data, depicted in Figure 1, show two peaks for all cases indicating two types of neighboring atoms.[16,17] Contributions of the two peaks were isolated from the distance (r) space with a smooth window (dashed curves) and back-transformed to k space. The resulting Fourier filtered EXAFS, truncated at 3 and 14.5 Å^{-1}, was employed in the curve fitting with the single electron scattering theory.

The two-term model used in the curve fitting is

$$k^3\chi(k) = B_L F_L(k_L) k_L{}^2 e^{-2\sigma_L{}^2 k_L{}^2} \frac{\sin[2k_L r_L + \phi_L(k_L)]}{r_L{}^2} + B_M F_M(k_M) k_M{}^2 e^{-2\sigma_M{}^2 k_M{}^2} \frac{\sin[2k_M r_M + \phi_M(k_M)]}{r_M{}^2} \quad (1)$$

where $F(k)$, $\phi(k)$, σ, r, and k denote the amplitude, the phase, the Debye–Waller factor, the distance, and the photoelectron wave vector, respectively. For the Mo (**1**) and the W (**2**) edges, L = S and M = Fe, whereas for the Fe edge, L = (S + Cl)/2 and M = Mo (**1**) or W (**2**). The scale factor B is related to the number of atoms N by $B = SN$ where S is the amplitude reduction factor which can be obtained from model compounds. The amplitude

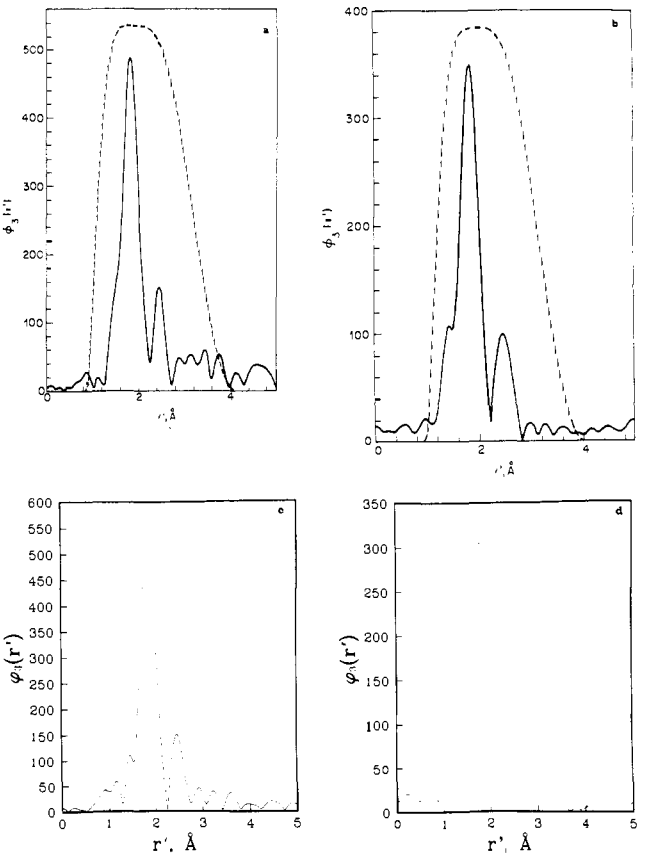

Figure 1. Fourier transforms of the transmissions EXAFS for (a) the Mo K-edge of $[Cl_2FeS_2MoS_2FeCl_2]^{2-}$ (**1**), (b) the Fe K-edge of $[Cl_2FeS_2MoS_2FeCl_2]^{2-}$ (**1**), (c) the W L_3-edge of $[Cl_2FeS_2WS_2FeCl_2]^{2-}$ (**2**), and (d) the Fe K-edge of $[Cl_2FeS_2WS_2FeCl_2]^{2-}$ (**2**).

(16) For details of the data analysis utilized in this paper, see ref 9 and 17g,h, as well as: Teo, B. K.; Shulman, R. G.; Brown, G. S.; Meixner, A. E. *J. Am. Chem. Soc.* **1979**, *101*, 5624.

(17) (a) Stern, E. A. *Contemp. Phys.* **1978**, *19*, 289. (b) Eisenberger, P.; Kincaid, B. M. *Science* **1978**, *200*, 1441. (c) Shulman, R. G.; Eisenberger, P.; Kincaid, B. M. *Annu. Rev. Biophys. Bioeng.* **1978**, *7*, 559. (d) Sandstrom, D. R.; Lytle, F. W. *Annu. Rev. Phys. Chem.* **1979**, *30*, 215. (e) Cramer, S. P.; Hodgson, K. O. *Prog. Inorg. Chem.* **1979**, *25*, 1. (f) Lee, P. A.; Citrin, P. H.; Eisenberger, P.; Kincaid, B. M. *Rev. Mod. Phys.* **1981**, *53*, 769. (g) Teo, B. K. *Acc. Chem. Res.* **1980**, *13*, 412. (h) Teo, B. K.; Joy, D. D., Eds. "EXAFS Spectroscopy: Techniques and Applications"; Plenum Press: New York, 1981.

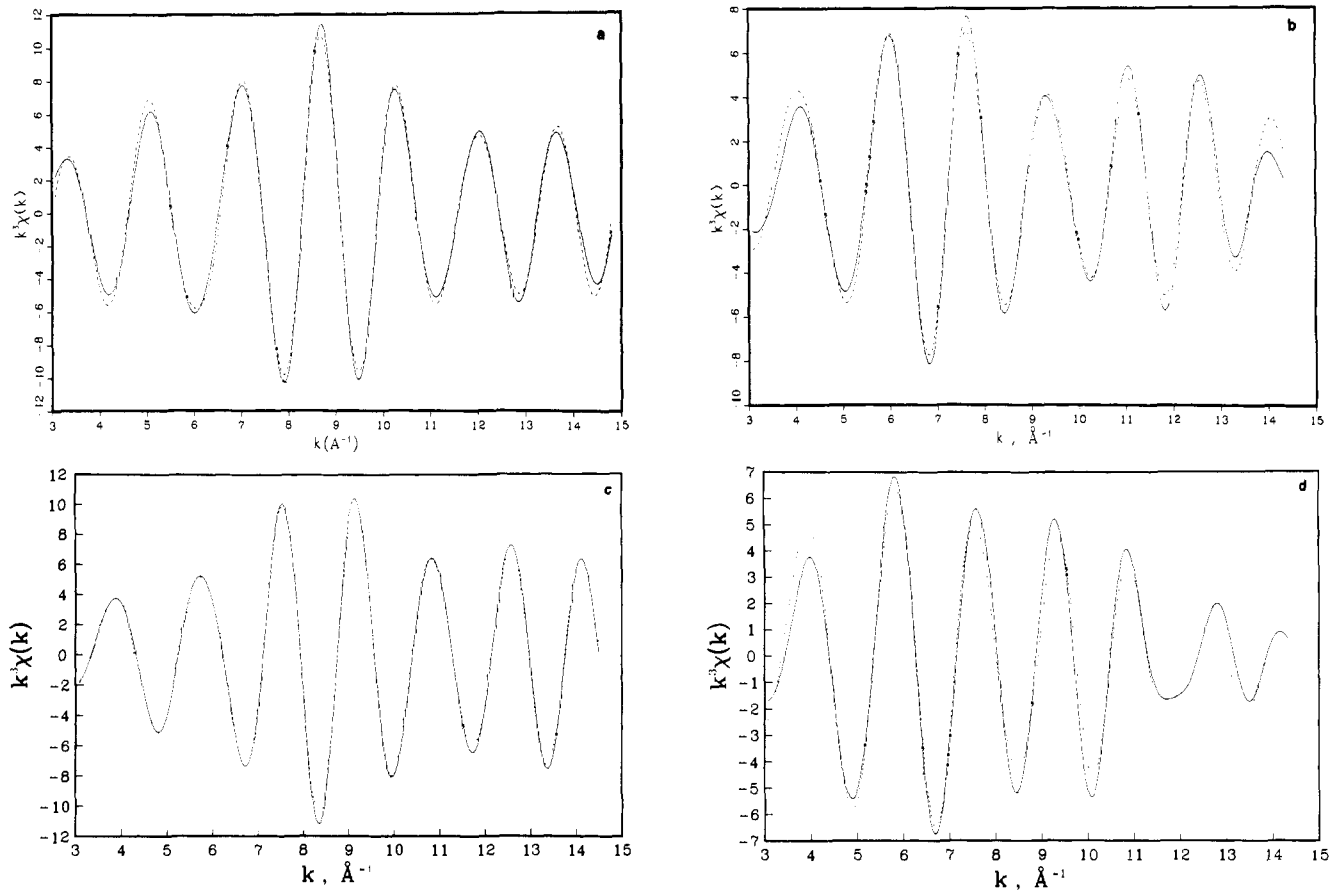

Figure 2. Fourier filtered EXAFS spectra (solid curves) and the best fits based upon theory (dashed curves) for (a) the Mo K-edge of **1**, (b) the Fe K-edge of **1**, (c) the W L_3-edge of **2**, and (d) the Fe K-edge of **2**.

$F(k)$ and the phase $\phi(k)$ functions employed were the theoretical curves tabulated by Teo and Lee.[18] For each k value, $F(k)$ and $\phi(k)$ were interpolated from the theoretical values.

Eight parameters were varied in the nonlinear least-squares refined curve fitting; the two scale factors, B_L and B_M, two Debye–Waller factors, σ_L and σ_M, two distances, r_L and r_M, and two threshold energy differences, ΔE_{0L} and ΔE_{0M}.[9,16,18] The results of best fits based on theory (BFBT) are tabulated in Table I and depicted in Figure 2. $\Delta E_0{}^P$ refers to the best fit threshold energy with reference to the edge position defined as the energy at half height of the edge jump.[9]

The coordination numbers presented in Table I were calculated at the fitted Debye–Waller factors, from both the best and restricted fit scale factors, according to $N = B/S$, using the amplitude reduction factors obtained from $S = s_0{}^2(1 - 5\sigma)$,[19] where $s_0{}^2 = 0.782$ for Mo, 0.80 for W, and 0.690 for Fe[20] and σ is the best fit Debye–Waller factor.

To improve the accuracy of the distances obtained from best fitting with theoretical $F(k)$ and $\phi(k)$ as well as to provide the amplitude reduction factors (S), a "fine adjustment" technique based on models (FABM) is applied to the best fit data.[9] The FABM technique relies upon a detailed exploration of the multidimensional parameter correlation space in the curve fitting, from which a simple method has been devised to alleviate parameter correlation problems. The method involves transferring the characteristic values of $\Delta E_0{}^*$, σ^*, and S^* from the model to the unknown systems for each type of interaction.

For the purpose of fine adjustment, the parameter correlations need to be investigated. As described elsewhere,[9] a series of fits were performed to reveal the correlations between $\Delta E_0{}^P$ and Δr, and between B and σ. The $\Delta E_0{}^P$ vs. Δr curves were then fitted with the equation

$$\Delta E_0{}^P = a_0 + a_1 \Delta r \tag{2}$$

and the B vs. σ curves were fitted with the equation

$$B = b_0 + b_1 \sigma + b_2 \sigma^2 \tag{3}$$

Here Δr represents the deviation of the distance from the best fit value. The resulting regression coefficients are tabulated in Table II. From a set of model compounds, the characteristic $\Delta E_0{}^*$, σ^*, and S^* values can be determined for each term (as average values).[9] These characteristic values can then be used to determine the distance adjustment $\Delta r = (\Delta E_0{}^* - a_0)/a_1$ (cf. eq 2) and the coordination number $N = B/S^* = (b_0 + b_1\sigma^* + b_2\sigma^{*2})/S^*$ (cf. eq 3).

The characteristic $\Delta E_0{}^*$, σ^*, and S^* values used in this paper were taken from the literature:[9,21] Mo–S, 1.89 eV, 0.061 Å, 0.585;

Table II. The Regression Coefficients[a] for the Linear $\Delta E_0{}^P$ vs. Δr Correlation and the Quadratic B vs. σ Correlation for $[Cl_2FeS_2MS_2FeCl_2]^{2-}$ where M = Mo (1) and W (2)

compd no.	A-B[b]	distance		coordination number		
		a_0, eV	a_1, eV/Å	b_0	b_1, Å^{-1}	b_2, Å^{-2}
1	Mo-S	7.122	222.809	1.623	1.811	327.440
	Mo-Fe	−4.106	211.670	0.332	−1.498	138.319
	Fe-S/Cl	8.105	209.540	1.169	1.786	244.535
	Fe-Mo	−7.074	205.354	0.231	−6.306	155.125
2	W-S	14.612	257.165	1.597	-3.672	414.338
	W-Fe	−1.364	205.845	0.329	-1.904	133.797
	Fe-S/Cl	4.022	187.430	0.946	1.597	217.250
	Fe-W	c	c	c	c	c

[a] The coefficients of determination, R^2, were 0.998–1.000. [b] A = absorber; B = backscatterer. [c] Cannot be determined (see text).

(18) Teo, B. K.; Lee, P. A. *J. Am. Chem. Soc.* **1979**, *101*, 2815.
(19) Teo, B. K., to be published.
(20) (a) Carlson, T. A.; Nestor, C. W., Jr.; Tucker, T. C.; Malik, F. B. *Phys. Rev.* **1968**, *169*, 27. (b) The $s_0{}^2$ value of 0.80 for Au was used for W since the latter was not available.

Table III. The FABM Interatomic Distances (r, Å) and Coordination Numbers (N) with Fitting Errors (in Parentheses), Distance Adjustments (Δr, Å), and Scale Factors (B) for $[Cl_2FeS_2MS_2FeCl_2]^{2-}$ where M = Mo (1) or W (2)

compd no.	A-B[a]	distance Δr	distance r	distance % error[b]	coordination number B	coordination number N	coordination number % error
1	Mo-S	−0.024	2.213 (9)	0.4	2.277	3.9 (7)	−2.7
	Mo-Fe	−0.003	2.766 (68)	−0.3	1.017	2.1 (11)	4.5
	Fe-S/Cl	−0.003	2.268 (21)	0.3	2.007	4.1 (10)	2.4
	Fe-Mo	0.012	2.780 (43)	0.2	0.534	1.0 (8)	−5.0
2	W-S	−0.012	2.210 (10)	0.1	1.819	4.0 (10)	−0.5
	W-Fe	0.029	2.789 (44)	−0.4	0.802	1.8 (13)	−8.4
	Fe-S/Cl	0.016	2.282 (24)	0.1	1.569	3.6 (12)	−9.4
	Fe-W	−0.040	2.781 (36)	−0.7	0.469	1.3 (7)	27.8

[a] A = absorber; B = backscatterer. [b] See Table I for the corresponding crystallographic distances.

Mo–Fe, −4.73 eV, 0.076 Å, and 0.487; Fe–S/Cl, 7.45 eV, 0.055 Å, 0.490; Fe–Mo, −4.79 eV, 0.069 Å, 0.562 for **1**, whereas W–S, 11.58 eV, 0.028 Å, 0.457; W–Fe, 4.48 eV, 0.067 Å, 0.438; Fe–S/Cl, 7.04 eV, 0.050 Å, 0.433; Fe–W, −1.48 eV, 0.054 Å, 0.367 for **2**. These characteristic values were obtained from (by averaging) an extensive series of M–Fe–S clusters containing MS_4 units (M = Mo, W) as tabulated elsewhere.[9,21] The FABM results are presented in Table III.

Results and Discussions

Fourier transforms of the $k^3\chi(k)$ vs. k data, depicted in Figure 1, show two peaks for Mo, W, and Fe edge EXAFS. The two peaks are interpreted as, in increasing distance, M–S, and M–Fe backscatterings for the M edge (Figure 1a,c), and Fe–S/Cl, and Fe–M backscatterings for the Fe edge (Figure 1b,d) of **1** (M = Mo) and of **2** (M = W).

The filtered $k^3\chi(k)$ data were fitted with a two-term model shown in eq 1 (vide supra). The best fit results are tabulated in Table I. Also included (second row of each term) are results from fits where the relative ratio of the scale factors for the two terms are restricted to the known values. In general, the two sets of results agree quite well. It is also evident from Table I that the distances determined by EXAFS agree with those obtained by single-crystal X-ray crystallography[12,13] to better than 1.5%. The Mo–Fe and the Fe–Mo distances obtained from the Mo and Fe K-edge EXAFS, respectively, are identical within experimental error. A somewhat larger discrepancy was obtained for the W–Fe and the Fe–W distances (2.760 (33) Å vs. 2.821 (65) Å) due to the fact that for the iron edge of **2**, the Fe–W term has a small EXAFS amplitude in the practical data range of 3–15 $Å^{-1}$.[18,22]

Further improvement in accuracy can be achieved by fine adjustment based on models (FABM). The parameter correlation curves and the results of FABM are tabulated in Tables II and III, respectively. (The regression coefficients for the Fe–W for **2** term cannot be given due to the small EXAFS contribution.) It is evident that FABM improves the accuracy of distance determination to better than 0.5% and the accuracy of coordination number determination to better than 9% (except, as expected, the weak Fe–W term in **2** which is off by 28%).

It is of interest to compare our EXAFS results of **1** and **2**. As can be seen from Tables II and III, the structural parameters and parameter correlation coefficients obtained from the EXAFS analysis of both the W and Fe data for **2** parallel closely those for the Mo and Fe EXAFS of **1**. The core dimensions of the W–Fe–S and Mo–Fe–S clusters are essentially identical (only small increases are observed for the W–Fe and bridging Fe–S distances of **2** vs. the Mo–Fe and bridging Fe–S distances of **1**).

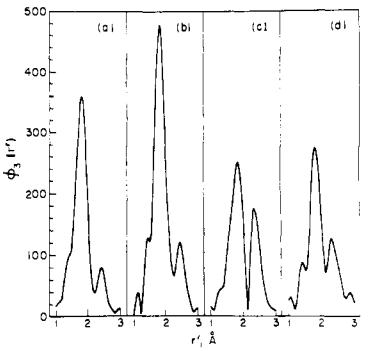

Figure 3. A comparison of the Fourier transforms of the Mo EXAFS $k^3\chi(k)$ spectra of $[S_2MoS_2Fe(SPh)_2]^{2-}$ (a),[9] $[Cl_2FeS_2MoS_2FeCl_2]^{2-}$ (b), and $[Mo_2Fe_6S_9(SEt)_8]^{3-}$ (c)[7] with that of the nitrogenase MoFe protein (d).[5]

The Fourier transforms of the Mo EXAFS of $[S_2MoS_2Fe(SPh)_2]^{2-}$,[9] $[Cl_2FeS_2MoS_2FeCl_2]^{2-}$ (this work), and $[Mo_2Fe_6S_9(SEt)_8]^{3-}$[7] as well as that of the Av MoFe protein[5] are compared in Figure 3. The former three-model compounds have one, two, and three iron atoms in the second coordination sphere of the Mo atoms. From the comparison shown in Figure 3, it is apparent that the Fourier transform of the MoFe protein EXAFS data is quite different from the model compounds as far as the peak intensities are concerned. Qualitatively, the Mo–S and Mo–Fe peaks in the MoFe protein Fourier transform resemble the corresponding peaks in the double-cubane clusters and **1**, respectively. The Mo–Fe distance of 2.76 Å in **1** is similar to that of 2.71 Å in the MoFe protein. By contrast, the Mo–S bond length in **1** is significantly shorter (Table I) than that in the MoFe protein. In nitrogenase, the EXAFS derived Mo–S distance of 2.35 Å[1,4] for the MoFe protein is very close to the Mo–S distance in the $[Mo_2Fe_6S_9(SEt)_8]^{3-}$ double cubane (2.340 Å) which contains a six-coordinate molybdenum in a +3.5 formal oxidation state.[5] In the $[(S_4)_2MoS]^{2-}$ anion[23] which contains a square-pyramidal Mo atom in a +4 formal oxidation state, two unequal, equatorial Mo–S bond lengths are found at 2.331 (1) and 2.387 (1) Å, with a mean value of 2.36 (3) Å. It is apparent that the formal oxidation state of the Mo atom in nitrogenase is lower than the formal oxidation state of the Mo in **1**. As a consequence, one might expect a coordination number greater than four for the Mo atom in the nitrogenase MoFe protein. The possibility exists that, in addition to the four S nearest neighbors, the Mo atom in nitrogenase is weakly bound to proximal donor atoms available within the site in the protein. In fact, a recent EXAFS study on the Fe–Mo cofactor[8] suggests that in addition to three or four S atoms at 2.35 Å from the Mo atom, there exist two or three oxygen or nitrogen ligands at 2.10 Å.

Acknowledgment. We thank Dr. D. Mills and the staff at Cornell High Energy Synchrotron Source (CHESS) for technical assistance and helpful consultations. We are also grateful to Virginia Bakirtzis for valuable assistance. DC and EDS acknowledge the support by a grant from NIH (GM-26671). M.R.A. was supported by a grant (to Prof. B. A. Averill) from the USDA/SEA Competitive Research Grants Office (5901-0410-8-0175-0).

Registry No. **1**·$(Ph_4P)_2$, 73621-80-4; **2**·$(Ph_4P)_2$, 73621-82-6; nitrogenase iron–molybdenum cofactor, 72994-52-6.

(21) Antonio, M. R., Ph.D. Thesis, Michigan State University, East Lansing, 1983.

(22) Theoretical calculations[18] showed that the tungsten backscattering amplitude has two dips at $k \approx 5$ and 10 $Å^{-1}$ and the amplitude is nearly 50% smaller than that of molybdenum within the data range of k = 3 to 13 $Å^{-1}$.

(23) Simhon, E. D.; Baenziger, N. C.; Kanatzidis, M.; Draganjac, M.; Coucouvanis, D.; *J. Amer. Chem. Soc.* **1981**, *103*, 1218.